VOL. 11, NO. 12, JUNE 2016 ISSN 1819-6608
ARPN Journal of Engineering and Applied Sciences

www.arpnjournals.com

CORROSION BEHAVIOUR OF HIGH VELOCITY OXYGEN FUEL SPRAY PROCESS AND ELECTRODEPOSITED COATING IN AQUEOUS ENVIRONMENT

Nur Amira Mohd Rabani and Z. Kamdi
Department of Materialand Design Engineering, Faculty of Mechanical and Manufacturing Engineering,
UniversitiTun Hussein Onn Malaysia, Parit Raja, BatuPahat, Johor, Malaysia
E-Mail: amira.mohdrabani@gmail.com

ABSTRACT

Cemented carbides are often referred to as "hard metals" due to the excellent combination of hardness and toughness characteristics. In order to increase the corrosion resistance and mechanical properties of the surfaces, cermet materials have been largely used for application on steels, generally using the high velocity oxygen fuel (HVOF) technique as well as the applications of electrodeposited composite coatings. This study compares the corrosion resistance of cermet based coatings which consist of WC-17%Co, WC-9%Ni, Ni electrodeposited coatings and Ni-SiC electrodeposited coatings. They were produced by two different methods of HVOF spraying process and eletrodeposition methods onto AISI 1018 steel plates. The microstructure of the coatings was examined by scanning electron microscope (SEM), energy dispersive spectroscopy (EDS) and X-ray diffraction (XRD). The coatings were characterized before and after corrosion test to evaluate the surface morphology. The hardness of the coatings also been investigated by using Vickers microhardness tester. Electrochemical polarization tests were performed in 0.5 M H_2SO_4 aqueous solution and 30% bentonite solution. Thus, the smallest grain size of 1.2522 µm were found in WC-9%Ni which is in agreement with its highest value of hardness which is 1625.37 HV. The WC-Co shows the highest corrosion rate in acidic environment with noticeably corroded appearance of the tested surface compare to other coatings. Ni-SiC electrodeposited coating shows the lowest corrosion rate of 4.287 mm/y in acidic medium while for bentonitesolution; WC-9%Ni coating shows the lowest corrosion rate of 0.0626 mm/y. It can be observed that this type of coatings have high corrosion resistance in respective environment. In conclusion, the corrosion resistance and hardness of the specimens are depends on the grain size of the coatings as well as composition of the coatings.

Keywords: cermet coating, corrosion, acidic environment.

INTRODUCTION

Electrodeposition is the application of metallic coatings to metallic or other conductive surfaces by electrochemical processes. This method is considered as ergonomic as it required less cost and occurred at room temperature to produce large area samples in industrial production (Narasimman *et al.*, 2012). While, the high velocity oxygen fuel (HVOF) spray process is a thermal spraying process in which fuel gas and oxygen are fed into a combustion chamber to produce a supersonic flame. Powder material is fed into this stream and accelerated to an extremely high velocity to generate a very dense and strong coating on the substrate (Aw *et al.*, 2008), (Wang *et al*., 2013). This technique has attracted much attention due to its capability to produce a high quality coating with a good adhesion quickly (Bolelli *et al.*, 2008), (Wu *et al*., 2012). Cermet based coatings considered as heterogenous materials with good mechanical properties and wide range of application often corroded due to preferential binder particles such as cobalt or nickel loss caused by the galvanic coupling effect in aggressive circumstance (Zhang *et al*., 2015). It can be produced in many ways, but for this studies it focused only by electrodeposition method and HVOF technique.

Conventional tungsten carbide hard materials consist of WC and a ductile binder phase. Tungstencarbide is corrosion resistant to nearly all kinds of medium, except forthe mixture of hydrofluoric acid and nitric acid (Jiang *et al.*, 2014). Cemented carbids have been widely used for a variety of machining, cutting, drilling, and other application due to its desired properties of heat resistance, abrasion resistance, and the good balance of hardness and toughness (Gu *et al*., 2015). The binder material provides toughness and adhesion for a coating. A binder with poor corrosion resistance in a service environment can cause delimination between coating and substrate (Cho *et al.*, 2006), (Aw *et al.*, 2008). Intrinsic defects such as porosities, microcracks, and oxide phases found in the coatings serve as sources for corrosion attack(Aw *et al*., 2008). It has been acknowledged that the microgalvanic corrosion, which markedly exacerbates the cobalt oxidation by the electron acceptors (i.e. oxygen, sulfide and phosphate) in acidic and neutral media, can occur between cobalt and hard phase due to the galvanic coupling effect (Zhang *et al*., 2015). Those defects can be minimized or partially eliminated by careful study of coating microstructure and control of processing parameters and thus improves its corrosion resistance. In fact, electroplating nickel coating has been widely used due to its excellent corrosion resistance, wear resistance, and particularly high hardness (Wang *et al.,* 2013). In other opinions, corrosion is an electrochemical charge transfer leads to material loss (Souza and Neville, 2005).Corrosion product films should be characterized to determine the corrosion mechanism and is significant in

the development of new corrosion protections (Bai *et al.*, 2014).

This paper reports the study of corrosion resistance of HVOF sprayed WC-17%Co and WC-9%Ni coatings with electrodeposited Ni and Ni-SiC coatings using electrochemical technique with 0.5 M H_2SO_4 aqueous solution and 30% bentonite solution as electrolyte. The surface morphology of the coatings before and after the testing were observed.

MATERIALS AND METHODS

Materials

The composition of the solution and operating parameters for electrodeposition are shown in Table-1. Analytical reagents and distilled water were used to prepare the plating solution. Cathode made of AISI 1018 low carbon steel of a size 10 mm x 10 mm x 1mm, were positioned in vertical plane with anode. A nickel plate of 50 mm x 50 mm was used as the anode. The distance between anode and cathode was 4 cm approximately. For each experiment, cathode was sequentially cleaned in ethanol, acetone, and distilled water before immersed in the plating bath to allow the electrodeposition process takes place.

Table-1. Composition and deposition parameters of electrodeposited plating bath used.

Deposition parameters	Amount
$NiSO_4$	250 g/L
$NiCl_2$	30 g/L
H_3BO_3	40 g/L
SiC	3 g/L
Distilled water	1000 ml
Temperature	30 ~ 35 ºC (room temperature)
Current density	50 mA/cm^2
Magnetic stirrer speed	250 rpm

Plates of AISI 1018 steel were coated by high velocity oxy-fuel (HVOF) spraying process with cobalt and nickel binder. Two commercially available WC-17%Co and WC-9%Ni coatings were used which supplied by an external vendor. The thickness of each layer was in the range of 150 µm to 300 µm. Then, the samples were cut into dimension of 10 mm x 10 mm x 10 mm by using wire cutting to ensure a well and smooth cutting process takes place for each type of cermet coatings. Followed by cold mounting by using epoxy and hardener, then grinding and polishing process to remove unwanted scratches and obtain finer and clear coating surface. Cold mounting at room temperature was chosen instead of hot mounting as to protect and ensure that the characteristics of the coatings are not affected.

Surface morphologies of all the coatings were examined by scanning electron microscope (SEM, Jeol 2000) operated at 10kV with energy dispersive spectroscopy (EDS). X-ray diffraction (XRD) was used to determine the phase present and the preferred orientation of the deposits. XRD was conducted with generator setting of radiation at 40kV and 40 mA. The scanning speed and scanning step were 2º/min and 0.02º with scan step time were 0.3 s, respectively. The range position start approximately at 20º and finished at around 60º to 80ºA computer-base search and match was used for phase identification by using EVA Software analysis. The hardness of the coatings were measured on a Vickers microhardness instrument at an applied load of 490.3 mN (HV 0.05) and indention time of 15 s with flat shape of test piece. Eight measurements were conducted on each sample and the mean were calculated.

Corrosion testing

The electrochemical behavior of the coated samples at room temperature was examined in aerated and unstirred 0.5 M H_2SO_4 aqueous solution and 3% bentonite solution. The samples was mounted by using a mixture of epoxy and hardener with an exposing area of 10mm^2 to the electrolyte. All the electrochemical tests were performed using AC potensiostat / galvanostat by ACM instruments. A standard three electrode cell was employed, with Ag/AgCl (3.5 M KCl, $E_{AgCl} = E_{SHE} - 200mV$) as the reference electrode, a graphite gauge as the counter electrode, and the samples were embedded as the working electrode. Potentiodynamic polarization tests were carried out at a scan rate of 1mV/s at room temperature. The scanning range starts from the initial potential of -250mV to the final potential of 250mV.Tafel extrapolation was used to determine the corrosion behavior of each sample in different environment of acidic and bentonite solution. The tests commenced after 30 minutes of free corrosion to allow full wetting of the coating surface and open circuit potential stabilization. The bentonitesolution was prepared by mixing 300 g of bentonite with 1000 mL of distilled water andwere stirred until a homogeneous solution was obtained. The mainmineral constituent in bentonite clay (Wyoming bentonite, MX-80) is sodium montmorillonite (75%) with a sheet-likecrystal structure as shown in Figure-1.

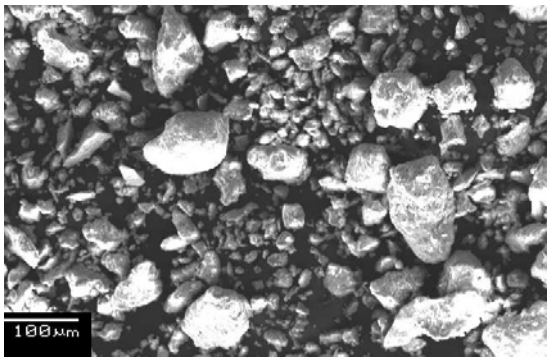

Figure-1. SEM image of as received powders of bentonite.

RESULTS AND DISCUSSIONS

SEM observation of coatings

The microstructural states of the coating system, before and after potentiodynamic polarization testing are illustrated in Figures 2, 3, 4 and 5. Based on Figures 2 (a) and 3 (a), it can be seen that the light contrast which indicates the carbide particles dissolve into the dark phases of cobalt and nickel phases. While for Figures 4 (a) and 5 (a), it reveals that the electrodeposited of pure nickel and SiC has exhibited irregular polyhedral crystal. This is parallel with the result obtained form the previously research(Vaezi *et al*, 2008). EDS analysis revealed the uniform distribution of SiC in the composite. After polarization testing, WC-Co interface appears as the most rough surface with protruding corrosion damage compared to other specimens in acidic environment. The corrosion occurs around the carbides grain boundaries, which is at the darker phases. Pitting-type corrosion occurred on the surface owing to the lack of enough compactness of the coatings (Jiang *et al*., 2014). This is a region which is richer with binder concentration of Co. As shown in Figure-2 (b), the appearance of cracked can be seen at the surface of coating, there is a possibility that these cracks could have been caused by dehydration of the surface film after its removal from the electrolyte and particularly in the high vacuum chamber of SEM (Lekatou *et al.*, 2008). It can be seen in Figure-5(b), Ni-SiC electrodeposited coating shows the less corroded damage towards acidic environment. This is due to the SiC particles which were embedded in the nickel coating, and filled in crevices, gaps and micron holes.

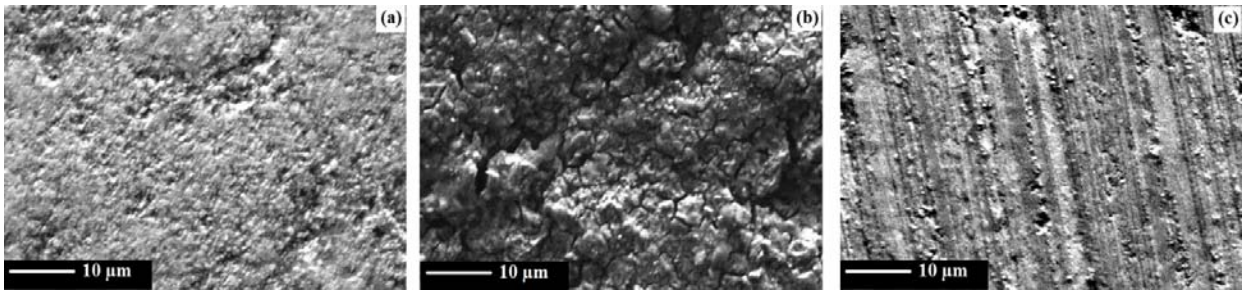

Figure-2. SEM micrographs of WC-Co surface coatings: (a) before test; (b) after corrosion test in H_2SO_4 aqueous solution; (c) after corrosion test in bentonite solution.

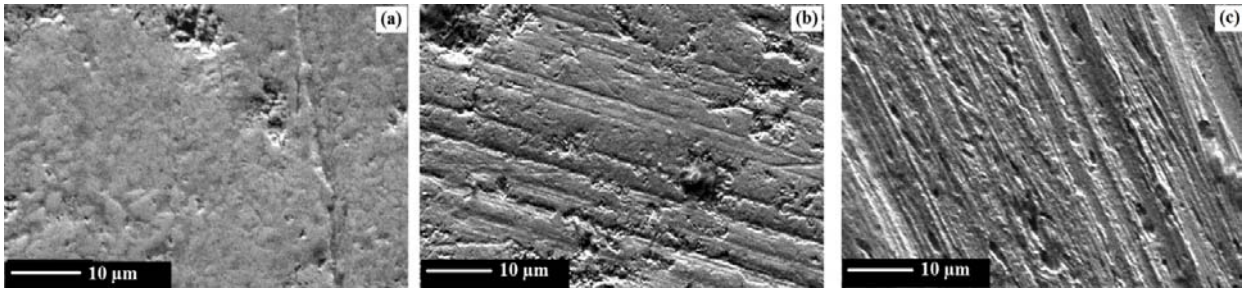

Figure-3. SEM micrographs of WC-Ni surface coatings: (a) before test; (b) after corrosion test in H_2SO_4 aqueous solution; (c) after corrosion test in bentonite solution.

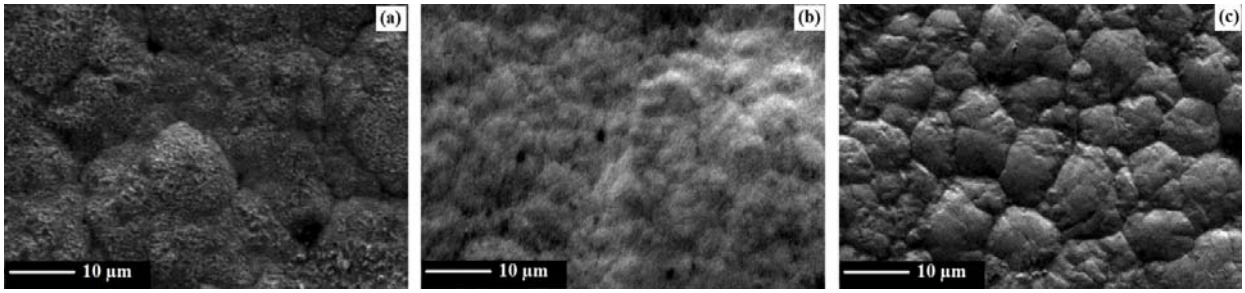

Figure-4. SEM micrographs of Ni-electrodeposited surface coatings: (a) before test; (b) after corrosion test in H_2SO_4 aqueous solution; (c) after corrosion test in bentonite solution.

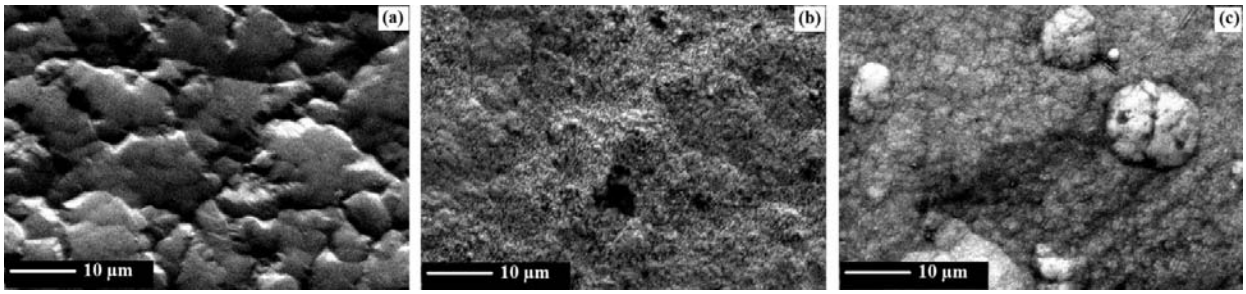

Figure-5. SEM micrographs of Ni-SiC electrodeposited surface coatings: (a) before test; (b) after corrosion test in H_2SO_4 aqueous solution; (c) after corrosion test in bentonite solution.

XRD characterization of coatings

The XRD method of Ni and Ni-SiC coatings are suitable method to determine the phase kind and presence of SiC particulates in the matrix. Figures 6 and 7 show the XRD diffraction of pure nickel and Ni-SiC composites. Based on Fig. 6, it has been proven that electrodeposited nickel coating is composed of mono-phase matrix. This result is parallel with the result obtained from the previous researchers (Vaezi *et al*., 2008), where the pure nickel deposit has exhibited an intense (200) diffraction line (ICDD file no. : 03-065-2865). However, the intensity of the diffraction peaks of the nickel in the Ni-SiC composite coatings is lower as shown in Figure-7. The growth of the electrodeposited layer takes place where a competition between the nucleation and crystal growth take place. In this case, SiC contribute more nucleation sides and thus retard the crystal growth causes the nickel matrix in the composite coating has a smaller grain size. Thus, this is attributed to the decrease in grain size of the Ni-SiC composite coating by the addition of SiC particles into the plating bath (Vaezi *et al*., 2008).

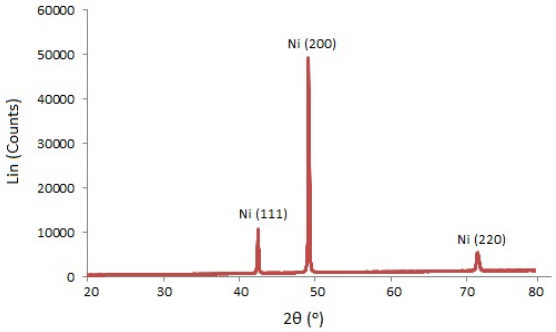

Figure-6. XRD pattern of Ni electrodeposited coating.

Figures 8 and 9 show XRD patterns of WC-Co and WC-Ni coatings respectively. The WC peaks are observed in both coatings, while W_2C, metallic W, and Ni phases are only observed in the XRD patterns for WC-Ni coating. The new phases observed are typical features of thermalspray coatings. This is due to the extremely high processing temperature in the process which resulted to the degradation of tungsten carbide coatings. This circumstances occurred due to the deformation of W_2C phase as a result of decarburization of WC which has been commonly observed (Aw *et al.*, 2008). This coating degradation cannot be avoided but can be minimized by controlling the processing parameters.

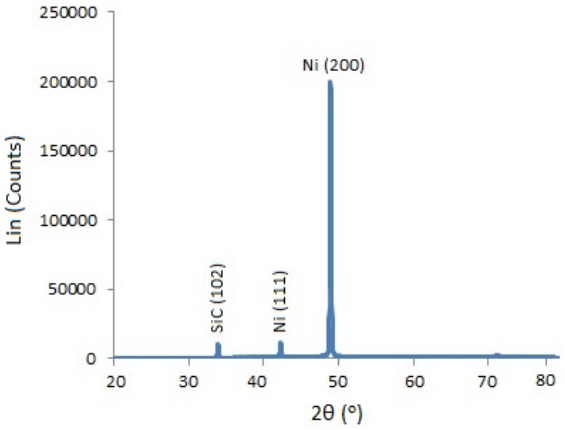

Figure-7. XRD pattern of Ni-SiC electrodeposited coating.

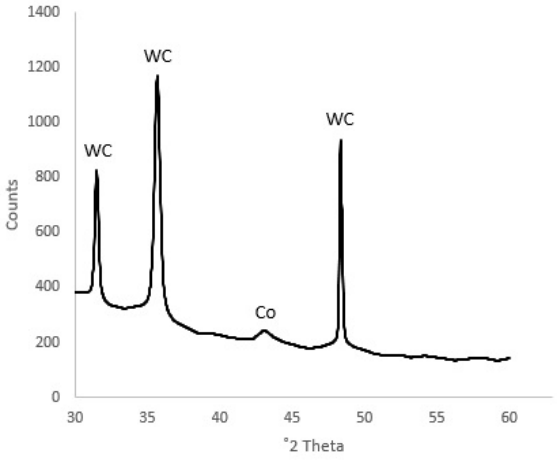

Figure-8. X-ray diffraction patterns of HVOF of WC-Co.

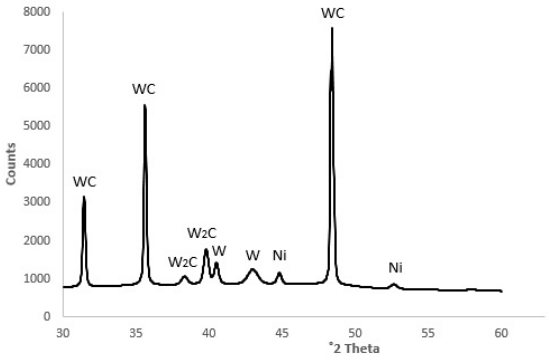

Figure-9. X-Ray diffraction patterns of HVOF of WC-Ni.

Potentiodynamic polarization

Figure-10 presents the typical Tafel polarization curves for the specimens coatings, immersed in 0.5 M H_2SOaqueous solution and 30% bentonite solution in room temperature. Table-2 and Table-3 present the data extracted from the Tafelcurve for 0.5 M H_2SO_4 aqueous solution and 30% bentonite solution respectively. In the present work, i_{corr} has been determined by the cathodic polarization data. As shown in Tables 2 and 3, it can be seen that the corrosion rate for all specimens in bentonite solution are lower compared to acidic solution. In bentonite solution, when an adherent clay layer appears to accumulate on the coating surface, the O_2 is rapidly consumed by reaction with minerals and organic matter in the clay achieving concentration at the coating surface (Kosec *et al*., 2015). Thus, under these anoxic conditions (a condition without oxygen), the corrosion damage that might occurred on the coating layers has been reduced compared to in acidic environment.

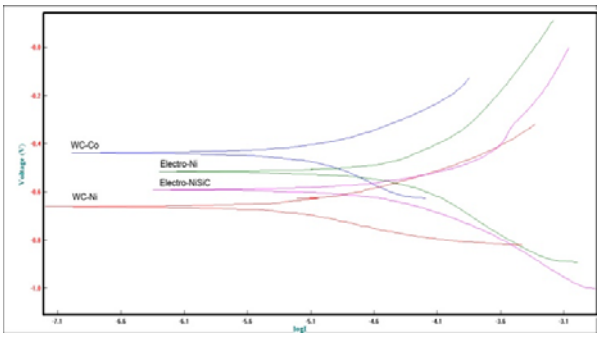

Figure-10. TypicalTafel curves for WC-Co, WC-Ni, Ni electrodeposited and Ni-SiC electrodeposited coatings.

Based on the data in Table-2, Ni-SiC electrodeposited coating has the lowest corrosion rate compared to other coatings in acidic environment. SiC were embedded in the nickel matrix and filled in crevices, gaps, and micron holes. Thus, it was reported that SiC which act as inert physical barriers to the initiation and development of defect corrosion, can improve the corrosion resistance of the coating (Vaezi *et al*., 2008). WC-Co shows the highest corrosion rate of 20.547 mm/y followed with WC-Ni of 6.689 mm/y. This is due to the fact that, WC-Co hardmetals are highly exposed to corroded due to preferential cobalt loss caused by the galvanic coupling effect in such particular environment (Zhang *et al*., 2015). This causes the coatings have a lower corrosion resistance. The corrosion behaviour of the WC-Co and WC-Ni composite could be affected by its components, the galvanic effect of the binder particles loss(Lekatou *et al*., 2008).

Table-2. Electrochemical results in 0.5 M H_2SO_4 aqueous solution.

Results	WC-17%Co	WC-9%Ni	Ni-Electrodeposited	Ni-SiC Electrodeposited
E_{corr} [V]	-385.612m	-398.638m	-313.081m	-398.251m
I_{corr} [A]	760.216µ	228.213µ	544.829µ	369.190µ
B_a	0.184	0.465	0.475	0.146
B_c	0.100	0.110	0.426	0.123
R_p	37.033	169.701	178.920k	78.531
Corrosion Rate, C_R [M/y]	808.823	263.323	219.648	168.757
Corrosion Rate, C_R [mm/y]	20.547	6.689	5.580	4.287

Table-3. Electrochemical results in 3% bentonite solution.

Results	WC-17%Co	WC-9%Ni	Ni-Electrodeposited	Ni-SiC Electrodeposited
E_{corr} [V]	-441.38m	-664.26m	-519.93m	-520.16m
I_{corr} [A]	1.8000µ	5.3833µ	99.979µ	68.465µ
B_a	297.86	119.75	708.83	379.80
B_c	539.64	121.01	566.77	485.74
Corrosion Rate, C_R [M/y]	8.2374	2.4636	45.755	31.333
Corrosion Rate, C_R [mm/y]	0.2092	0.0626	1.1622	0.7958

Thickness and hardness

Table-4 shows the variation in the thickness and hardness of the specimen coatings. It is found that for HVOF sprayed technique, WC-Ni has a higher hardness compared to WC-Co. While for electrodeposited technique, Ni-SiC coating has a higher hardness compared to Ni coating. This is parallel to the result obtained for thegrain size of Ni-SiC electrodeposited coating which is 12.5175 µm, smaller than the Ni electrodeposited coating of 13.2829 µm. Based on (Vaezi *et al.*, 2008), it has been reported that the existence of SiC particles deposited in the nickel matrix are tend to restrain the growth of the nickel grains and the plastic deformation of the matrix under a loading, by way of grain fining and dispersive strengthening effects.

Table-4. Thickness and hardness of the coatings.

Samples	Average hardness [HV]	Thickness (µm)
WC-Co	**1309.95**	**305.59**
WC-Ni	1625.37	151.12
Ni electrodeposited	313.466	251.36
Ni-SiC electrodeposited	280.510	257.70

CONCLUSIONS

Cermet based coatings can be successfully produced by both techniques of HVOF sprayed process and electrodeposited method. It shows that SiC particulates can be successfully co-deposited with nickel by electrodeposition process. This is prove by the result obtained from the electrochemical test that the Ni-SiC electrodeposited coating shows the lowest corrosion rate compared to other coatings. Eventhough, during the electrodeposited process, agglomeration slightly occurred. The Ni-SiC composite coatings have a higher microhardness than the pure nickel coating. This is due to the grain-fining and dispersive strengthening effects of the deposited hard SiC particles. The Ni-SiC electrodeposited coating has grain size of 12.5175 µm which is slightly smaller than the Ni electrodeposited coating of 13.2829 µm.

Meanwhile, WC-Ni shows a better corrosion resistance with a higher microhardness compared to WC-Co. This might due to the grain size of WC-Ni which is 1.2522 µm smaller than WC-Co of 1.6837 µm. The results obtained parallel to a formula of Hall-Petch law (HPL); the microhardness of coatings will increase with the refinement of grain size.

REFERENCES

Aw, P. K., Tan, A. L. K., Tan, T. P. and Qiu, J. 2008. Corrosion resistance of tungsten carbide based cermet coatings deposited by High Velocity Oxy-Fuel spray process. Thin Solid Films, 516(16), pp. 5710-5715.

Bai, P., Zheng, S., Zhao, H., Ding, Y., Wu, J. and Chen, C. 2014. Investigations of the diverse corrosion products on steel in a hydrogen sulfide environment. Corrosion Science, 87(0), pp. 397-406.

Bolelli, G., Lusvarghi, L. and Giovanardi, R. 2008. A comparison between the corrosion resistances of some HVOF-sprayed metal alloy coatings. Surface and Coatings Technology, 202(19), pp. 4793-4809.

Cho, J. E., Hwang, S. Y. and Kim, K. Y. 2006. Corrosion behavior of thermal sprayed WC cermet coatings having various metallic binders in strong acidic environment. Surface and Coatings Technology, 200(8), pp. 2653-2662.

Gu, L., Huang, J., Tang, Y., Xie, C. and Gao, S. 2015. Influence of different post treatments on microstructure and properties of WC-Co cemented carbides. Journal of Alloys and Compounds, 620, pp. 116-119.

Jiang, Y., Yang, J. F., Xie, Z. M., Gao, R. and Fang, Q. F. 2014. Corrosion resistance of W–Cr–C coatings fabricated by spark plasma sintering method. Surface and Coatings Technology, 254, pp. 202-206.

Kosec, T., Qin, Z., Chen, J., Legat, A. and Shoesmith, D. W. 2015. Copper corrosion in bentonite/saline groundwater solution: Effects of solution and bentonite chemistry. Corrosion Science, 90, pp. 248-258.

Lekatou, A., Regoutas, E. and Karantzalis, A. E. 2008. Corrosion behaviour of cermet-based coatings with a bond coat in 0.5M H2SO4.Corrosion Science, 50(12), pp. 3389-3400.

Narasimman, P., Pushpavanam, M. and Periasamy, V. M. 2012. Wear and scratch resistance characteristics of electrodeposited nickel-nano and micro SiC composites. Wear, 292-293, pp. 197-206.

Souza, V. A. D. and Neville, A. 2005. Corrosion and synergy in a WCCoCr HVOF thermal spray coating-understanding their role in erosion–corrosion degradation. Wear, 259(1-6), pp. 171-180.

Vaezi, M. R., Sadrnezhaad, S. K. and Nikzad, L. 2008. Electrodeposition of Ni-SiC nano-composite coatings and evaluation of wear and corrosion resistance and electroplating characteristics. Colloids and Surfaces A: Physicochemical and Engineering Aspects. 315(1-3), pp. 176-182.

Wang, D., Cheng, Y., Jin, H., Zhang, J. and Gao, J. 2013. Influence of LaCl3 addition on microstructure and properties of nickel-electroplating coating. Journal of Rare Earths. 31(2), pp. 209-214.

Wang, L. J., Qiu, P.-x., Liu, Y., Zhou, W.-x., Gou, G.-q. and Chen, H. 2013. Corrosion behavior of thermal sprayed WC cermet coatings containing metallic binders in saline environment. Transactions of Nonferrous Metals Society of China. 23(9), pp. 2611-2617.

Wu, Y., Hong, S., Zhang, J., He, Z., Guo, W., Wang, Q. and Li, G. 2012. Microstructure and cavitation erosion behavior of WC–Co–Cr coating on 1Cr18Ni9Ti stainless steel by HVOF thermal spraying. International Journal of Refractory Metals and Hard Material, 32, pp. 21-26.

Zhang, Q., He, Y., Wang, W., Lin, N., Wu, C. and Li, N. 2015. Corrosion behavior of WC-Co hardmetals in the oil-in-water emulsions containing sulfate reducing Citrobacter sp. Corrosion Science. 94, pp. 48-60.